View metadata, citation and similar papers at core.ac.uk

brought to you by CORE

provided by Ghent University Academic Bibliography

Journal of General Virology (2007), **88**, 2527–2532 DOI 10.1099/vir.0.82991-0

Short Communication

Attachment and internalization of feline infectious peritonitis virus in feline blood monocytes and Crandell feline kidney cells

Evelien Van Hamme, Hannah L. Dewerchin, Els Cornelissen and Hans J. Nauwynck

Laboratory of Virology, Faculty of Veterinary Medicine, Ghent University, 9820 Merelbeke, Belgium

Correspondence
Hans J. Nauwynck
hans.nauwynck@ugent.be

Received 9 March 2007
Accepted 21 May 2007

In this study, kinetics of attachment and internalization of feline infectious peritonitis virus (FIPV) serotype I strain Black and serotype II strain 79-1146 were determined in feline monocytes from two cats and in Crandell feline kidney (CrFK) cells. Attached FIPV I (Black) particles were observed on almost all monocytes. Within 1 h, 17 particles were bound per cell and, within 1 min, 89 % of the bound particles were internalized. For FIPV II (79-1146), attachment was observed on 66 and 95 % of all monocytes from the two cats. After 1 h, respectively five and 20 particles were bound per cell (all cells considered). Within 1 min, 60 % of the bound particles were internalized. Internalization in monocytes was efficient and proceeded via endocytosis. In CrFK cells, attachment and internalization were less efficient, especially for FIPV I (Black), so this cell line is not suitable for studying FIPV entry.

Feline infectious peritonitis virus (FIPV) is a coronavirus belonging to the order *Nidovirales* (Cavanagh, 1997; Cowley *et al.*, 2000; Gorbalenya *et al.*, 2006). Based on comparative sequence analysis, human coronavirus 229E (HCoV 229E), porcine transmissible gastroenteritis virus (TGEV), porcine epidemic diarrhea virus, canine coronavirus (CCoV) and feline coronaviruses (FCoV) are grouped in phylogenetic group 1 (González *et al.*, 2003; Spaan *et al.*, 2005; Gorbalenya *et al.*, 2006). Feline coronaviruses are divided into two serotypes: serotype I and the less prevalent serotype II (Pedersen *et al.*, 1984; Hohdatsu *et al.*, 1992). Type II strains are related closely to CCoV and TGEV (Pedersen *et al.*, 1983) and are thought to be recombinants of type I strains and CCoV (Vennema *et al.*, 1995). Unlike type I strains, type II strains grow easily in cell culture, such as Crandell feline kidney (CrFK) cells, and are therefore used frequently in FIPV studies.

Aminopeptidase N (APN) serves as a receptor for several group 1 coronaviruses (Tresnan *et al.*, 1996), including HCoV 229E (Yeager *et al.*, 1992), porcine respiratory coronavirus and TGEV (Delmas *et al.*, 1992, 1993, 1994). For both serotype I and II FCoVs, stably expressed APN cDNA isolated from the *Felis catus* whole fetus (fcwf) cell line induced susceptibility in FCoV-resistant cells. Although strains of both serotypes were able to infect these cells, the efficiency of infection was different (Tresnan *et al.*, 1996). Hohdatsu *et al.* (1998) showed that only serotype II strains of FCoV use feline APN (fAPN) as a receptor for internalization into feline cell lines. Infection of bone marrow-derived macrophages with FIPV II (79-1146) was restricted from approximately 33 to 3 % of cells by a mAb against fAPN (Rottier *et al.*, 2005). Whether fAPN is the receptor for FIPV II on *in vivo* target cells, feline blood monocytes, is not known. The receptor for FIPV I has not been identified.

Viruses may enter cells via two pathways. Viral envelopes may fuse with the plasma membrane or with endosomal membranes after entering cells via endocytosis. Several group 1 coronaviruses enter cells via endocytosis: HCoV 229E (Nomura *et al.*, 2004), TGEV (Hansen *et al.*, 1998) and CCoV (Savarino *et al.*, 2003). Mouse hepatitis virus, a group 2 coronavirus, enters cells by both endosomal and non-endosomal pathways. The pathway of internalization was shown to depend upon the virus strain and the nature of the cell being infected (Kooi *et al.*, 1991; Nash & Buchmeier, 1997). Internalization of FIPV has not been studied in either primary cells or cell lines.

In this study, kinetics of attachment and internalization were studied for FIPV in feline blood monocytes, the primary target cells, and compared with those in CrFK cells, used frequently as a model cell line for FCoV–cell interactions. Further, it was investigated whether FIPV enters monocytes and CrFK cells via fusion with the plasma membrane or via endocytosis.

Monocytes were isolated from blood collected from two FCoV-, feline leukemia virus- and feline immunodeficiency virus-negative cats as described previously (Dewerchin *et al.*, 2005) and seeded on glass coverslips. The adherent

A figure showing co-localization of biotinylated particles and FIPV virions is available with the online version of this paper.

cells consisted of 86 ± 7 % monocytes [assessed with monocyte marker DH59B; Veterinary Medical Research and Development (VMRD)]. Experiments were performed at 36 h post-seeding, using third passages of type I FIPV strain Black (Black, 1980) on fcwf cells and third passages of type II FIPV strain 79-1146 (McKeirnan *et al.*, 1981) on CrFK cells. Both strains were kindly provided by Dr H. F. Egberink (Utrecht University, The Netherlands). Virus purification was performed as described by Delputte *et al.* (2002) and Delputte & Nauwynck (2004). Purified virus was biotinylated with Sulfo-NHS-LC-Biotin (Pierce) according to the manufacturer's instructions. Purified viral-particle suspension (200 µg) was applied to $10^{4.4}$ monocytes or 10^6 CrFK cells throughout the experiments. Application of diluted samples of biotinylated virus suspension to streptavidin-coated coverslips (Xenopore) and staining with fluorescein isothiocyanate (FITC)-labelled streptavidin (Molecular Probes) showed that this amount of virus contains 7.9×10^9 FIPV I (Black) particles and 5.0×10^{10} FIPV II (79-1146) particles. Double staining with polyclonal anti-FIPV–FITC (VMRD) and streptavidin–Texas red (Molecular Probes) confirmed the concurrence of biotin and FIPV antigens (see Supplementary Fig. S1, available in JGV Online). Further, it was shown that the biotinylation procedure did not influence the obtained kinetics (data not shown). Cell vitality was checked at the end of the experiments. Triplicate assays were performed and kinetics were compared by using the Wilcoxon signed ranks (WSR) test from the SPSS software package (version 12.0; SPSS Inc.).

To determine kinetics of attachment, cells were chilled on ice for 15 min and inoculated with biotinylated FIPV I (Black) or II (79-1146) at 4 °C. At different time points, cells were washed with PBS and fixed with 1 % formaldehyde. Attached particles were visualized by using FITC-labelled streptavidin and counted manually for 50 randomly chosen cells by means of a DM IRB inverted microscope (Leica). Fig. 1(a) illustrates the origin of the graphs shown in Fig. 1(b). FIPV I (Black) bound to almost all monocytes (98.8 % of the monocytes for cat 1 and 99.5 % for cat 2). For cat 1, the number of attached

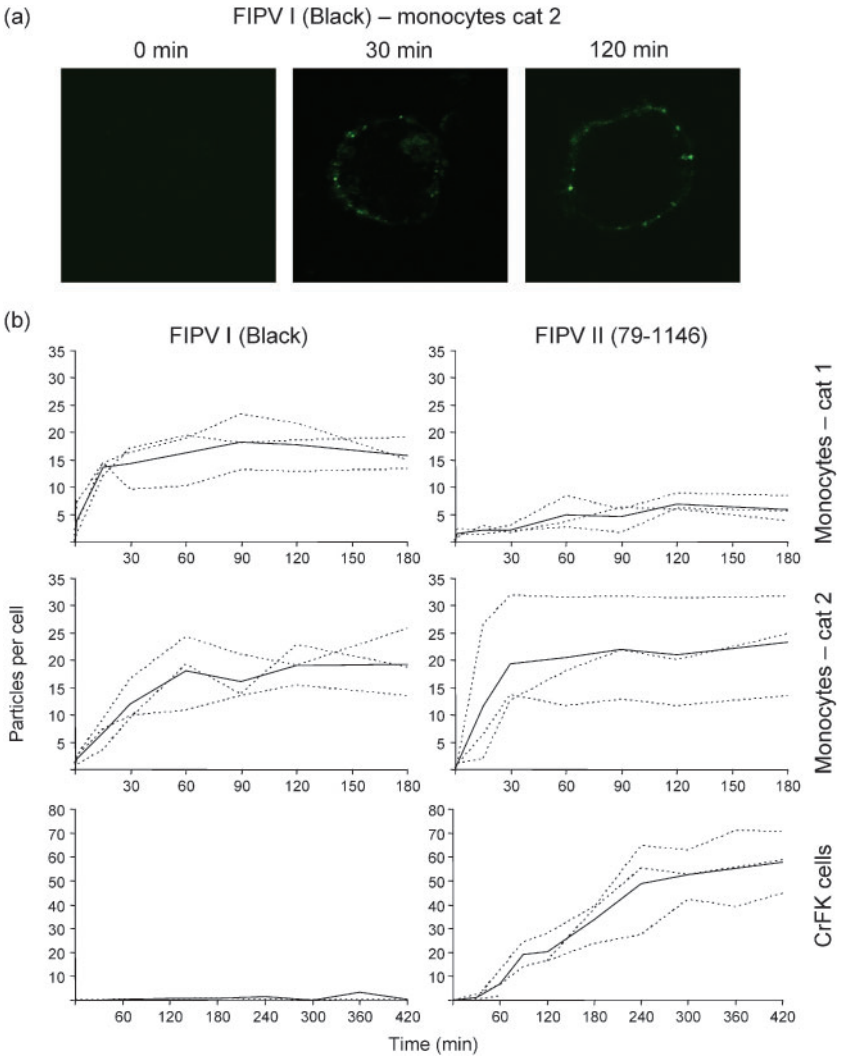

Fig. 1. Kinetics of attachment. (a) Cells were inoculated with biotinylated FIPV and incubated at 4 °C. At designated time points, virus was visualized by using streptavidin–FITC. (b) Dotted lines depict time courses determined in three independently performed experiments; the solid line depicts the mean time course based on these three experiments.

particles per cell reached 14±1 after 15 min; for cat 2, it was 18±1 after 1 h. Thereafter, no further increase was observed. Attachment to CrFK cells was restricted to 15.4 % of the cells and, after 2 h, only 1±1 particle was bound per cell (all cells considered). FIPV II (79-1146) bound to only 66.2 % of the monocytes for cat 1 and to 95.0 % for cat 2. For cat 1, the number of attached particles per cell increased slowly to 5±3 during the first hour. For cat 2, a strong increase to 19±10 particles per cell was observed during the first 30 min. Afterwards, attachment remained at the same level. Clearly, cat 2 reached a higher level of attached FIPV II (79-1146) particles than cat 1. In contrast to the results for FIPV I (Black), almost all CrFK cells (99.8 %) bound FIPV II (79-1146) particles. Also, more particles were attached, although the kinetics were slow. During 4 h incubation, the number of bound particles per cell increased gradually to 49±19. Longer incubation times increased the amount of bound virus slightly. Based on the numbers of inoculated and attached virus particles, it is clear that virus was present in excess in all experiments. So, for both FIPV I (Black) and II (79-1146), all possible binding sites were taken.

To determine the kinetics of entry, cells were incubated with virus until the maximum number of attached particles was reached, i.e. 1 h for incubation of monocytes with both strains, and 2 and 5 h for incubation of CrFK cells with respectively FIPV I (Black) and FIPV II (79-1146) (Fig. 1). Cells were washed and plates were transferred from 4 to 37 °C (time point zero for the kinetics of internalization). Then, cells were fixed at different time points. Attached particles were visualized by using streptavidin–Texas red. After permeabilizing cells with 0.1 % Triton X-100, internalized particles were stained with streptavidin–FITC. Kinetics of internalization are shown in Fig. 2. The percentages given were calculated by quantifying particles inside the cytosol and on the surface of 10 cells with attached and/or internalized particles. The kinetics of internalization for FIPV I (Black) in monocytes were similar for both cats. Almost all monocytes that bound FIPV I (Black) virions

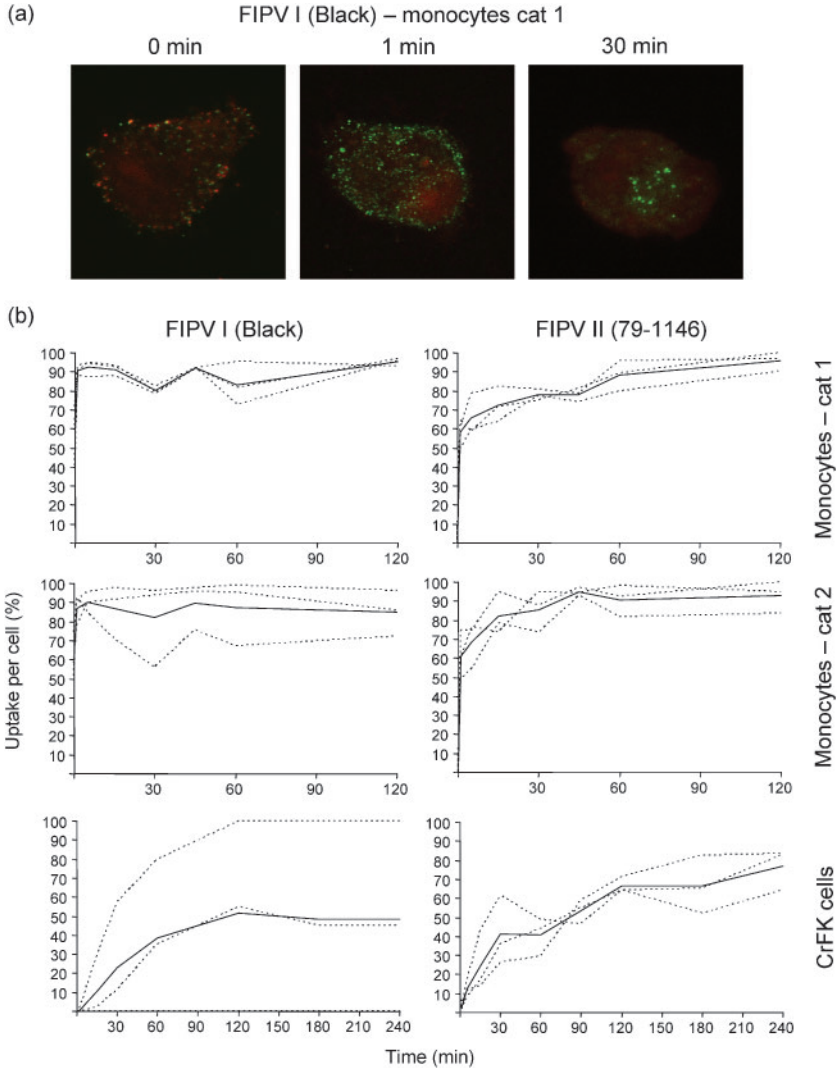

Fig. 2. Kinetics of internalization. (a) Cells were inoculated with biotinylated FIPV and incubated at 4 °C until saturation of attachment. Plates were then transferred to 37 °C. At designated time points, virus at the plasma membrane was visualized by using streptavidin–Texas red and, after permeabilization, internalized virus was visualized by using streptavidin–FITC. (b) Dotted lines depict time courses determined in three independently performed experiments; the solid line depicts the mean time course based on these three experiments.

internalized virions (98.9 % of the monocytes for cat 1 and 98.5 % for cat 2). Remarkably, immobilization of the cells at 4 °C could not inhibit internalization completely, as there were already particles internalized at time point zero. Within the first minute, 89±6 % of the bound particles were internalized per cell. This level of internalization was roughly maintained, although a slight, not significant, decrease to 85±13 % was observed after 1 h. However, unlike for monocytes, uptake was restricted in CrFK cells to 20.8 % of the cells that had bound virus or only 3.2 % of all cells. No internalization was observed after the first minute, but during the first 2 h, kinetics gradually increased to a maximum, with 52 % of the bound particles internalized per cell. The percentages of internalized particles per cell varied between 0 and 100 %, as often only one particle was bound, so only one particle could be internalized. As for FIPV I (Black), internalization of FIPV II (79-1146) was mediated by nearly all monocytes that had bound virus particles (92.5 % of the analysed monocytes from cat 1 and all analysed monocytes from cat 2) and kinetics were similar for both cats. After 1 min, a mean of 60±9 % of the bound virions were internalized per cell. Internalization further increased gradually up to 90±7 % after 1 h. All CrFK cells were capable of internalizing FIPV II (79-1146) virions. Within the first minute, only 3±2 % of the bound particles were internalized. However, the percentage of internalization per cell increased gradually to 67±4 % after 2 h. Longer incubation times increased the percentage of internalization per cell only slightly.

The kinetics of internalization indicate that the majority of bound FIPV particles enter cells via endocytosis, as biotinylated envelopes were present inside the cell. However, a small fraction of biotinylated material remained outside the cell. This could be bound virus particles, unable to enter the cell, or biotinylated envelopes, left behind after fusion with the host-cell membrane. To determine the nature of the material left at the plasma membrane, cells were chilled on ice, inoculated and incubated at 4 °C. After attachment, cells were shifted to 37 °C. Cells were fixed when maximal uptake was reached (after 1 and 2 h incubation at 37 °C for monocytes and CrFK cells, respectively) and remaining material at the plasma membrane was stained with polyclonal anti-FIPV–FITC. After permeabilizing cells, nucleocapsid proteins were stained with the mAb E22-2 (kindly provided by Dr T. Hohdatsu, Kitasato University, Japan) and visualized with goat anti-mouse–Texas red (Molecular Probes). Fig. 3 shows that all FIPV material at the plasma membrane co-localized with nucleocapsid proteins. Thus, the biotinylated material consisted of intact virions. This implies that, under the present experimental conditions, both FIPV strains enter monocytes exclusively via endocytosis, and FIPV II (79-1146) also does so in CrFK cells.

In this study, the initial steps in FIPV infection were analysed in target cells by determining kinetics of attachment and internalization. Kinetics of attachment for FIPV II (79-1146) were significantly different between the two cats (P=0.025; WSR). This difference could be the

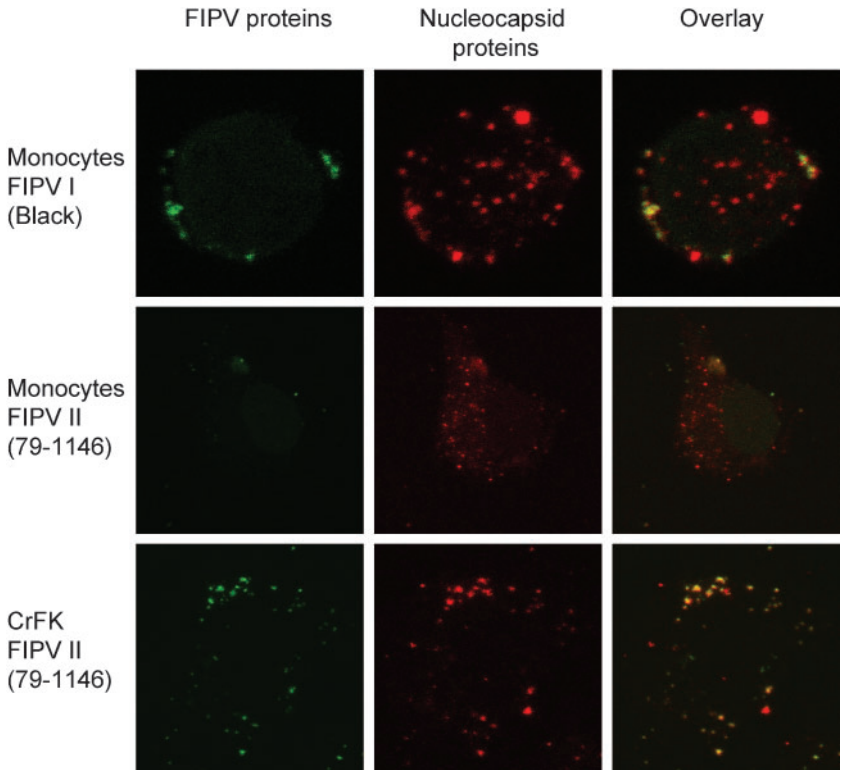

Fig. 3. Co-localization of non-internalized biotinylated material and FIPV nucleocapsid protein. Confocal images of monocytes and CrFK cells that were incubated at 4 °C, then transferred to and left at 37 °C until uptake was completed are shown. Biotinylated material was stained with α-FIPV–FITC and nucleocapsid protein with mAb E22-2 and goat α-mouse–Texas red.

consequence of variable expression levels of a cellular component involved in attachment, e.g. a specific serotype II FIPV receptor. Another difference in kinetics of attachment was observed between FIPV I (Black) and FIPV II (79-1146) for the monocytes of cat 1 ($P=0.012$; WSR) and cat 2 ($P=0.036$; WSR). This could indicate that type I and II strains use different receptors on monocytes and that the serotype II receptor may be expressed differentially between cats, whereas the serotype I receptor is apparently not. Differences in receptor between type I and II have previously been demonstrated in cell culture (Hohdatsu *et al.*, 1998). As only two cats were considered, these data cannot lead to general conclusions. Further research will focus on the receptors of FIPV in monocytes, which will allow interpretation of the present findings.

Internalization in monocytes was very efficient for both serotypes and was mediated exclusively by endocytosis. The efficiency of internalization of TGEV and HCoV 229E, also group 1 coronaviruses, and of porcine reproductive and respiratory syndrome virus (PRRSV), another member of the order *Nidovirales*, in macrophages is comparable to that of FIPV in monocytes (Hansen *et al.*, 1998; Nauwynck *et al.*, 1999; Nomura *et al.*, 2004). Other mutual observations between TGEV, PRRSV and FIPV are the accumulation of particles in endosomes (already occurring 15 min after the start of virus uptake for FIPV) and the decreasing number of particles inside the cell, due to particle disassembly, at later time points in the kinetics (within 1 h for FIPV). The decreasing number of particles explains the apparent drop in internalization described for FIPV I (Black), where the percentages of uptake per cell were higher after 1 min than after 1 h.

Replication of FIPV is limited to a small fraction (<1 % for FIPV 79-1146) of monocytes (Dewerchin *et al.*, 2005) and peritoneal macrophages (Morahan *et al.*, 1985; Stoddart & Scott, 1989). However, virus binding and uptake took place in almost all monocytes. Thus, the mechanism behind the resistance of most monocytes/macrophages must lie in inhibition of genome release and/or translation. Similar observations were obtained for PRRSV replication in alveolar macrophages (Duan *et al.*, 1997; Nauwynck *et al.*, 1999).

Attachment and internalization of FIPV I (Black) in CrFK cells were very inefficient. It is possible that no specific mechanism is involved. Particles may accidentally co-internalize with other compounds. The ability of FIPV I (Black) to induce infection of CrFK cells was restricted to only 0.003 % of the cells at 12 h post-inoculation. Infectivity of FIPV I (Black) in CrFK cells is the subject of contradictory literature. Black (1980) reported susceptibility of CrFK cells, whereas Hohdatsu *et al.* (1998) failed to induce infection. It is possible that susceptibility of CrFK cells may differ due to genetic changes during long-term subpassaging. CrFK cells are often used as a model cell line for FIPV serotype II infection studies. However, internalization of FIPV II (79-1146) was slower and less efficient than in monocytes. Thus, FIPV seems to interact differently with CrFK cells and with monocytes. This confirms earlier observations (Dewerchin *et al.*, 2005). It is concluded that the CrFK cell line is not suitable for studying FIPV entry into target cells.

The findings concerning attachment and internalization in monocytes are useful for further characterization of the FIPV entry process. Unravelling this mechanism may lead to new targets for drug development.

Acknowledgements

We are grateful to Dr T. Hohdatsu and Dr H. F. Egberink for supplying antibodies and virus strains. E. V. H. was supported by a doctoral grant from the special research fund of Ghent University (01D29005) and H. L. D. and E. C. by the Institute for the Promotion of Innovation through Science and Technology in Flanders (IWT Vlaanderen).

References

Black, J. W. (1980). Recovery and in vitro cultivation of a coronavirus from laboratory-induced cases of feline infectious peritonitis (FIP). *Vet Med Small Anim Clin* **75**, 811–814.

Cavanagh, D. (1997). *Nidovirales*: a new order comprising *Coronaviridae* and *Arteriviridae*. *Arch Virol* **142**, 629–633.

Cowley, J. A., Dimmock, C. M., Spann, K. M. & Walker, P. J. (2000). Gill-associated virus of *Penaeus monodon* prawns: an invertebrate virus with ORF1a and ORF1b genes related to arteri- and coronaviruses. *J Gen Virol* **81**, 1473–1484.

Delmas, B., Gelfi, J., L'Haridon, R., Vogel, L. K., Sjöström, H., Norén, O. & Laude, H. (1992). Aminopeptidase N is a major receptor for the enteropathogenic coronavirus TGEV. *Nature* **357**, 417–419.

Delmas, B., Gelfi, J., Sjöström, H., Norén, O. & Laude, H. (1993). Further characterization of aminopeptidase N as a receptor for coronaviruses. *Adv Exp Med Biol* **342**, 293–298.

Delmas, B., Gelfi, J., Kut, E., Sjöström, H., Norén, O. & Laude, H. (1994). Determinants essential for the transmissible gastroenteritis virus-receptor interaction reside within a domain of aminopeptidase N that is distinct from the enzymatic site. *J Virol* **68**, 5216–5224.

Delputte, P. L. & Nauwynck, H. J. (2004). Porcine arterivirus infection of alveolar macrophages is mediated by sialic acid on the virus. *J Virol* **78**, 8094–8101.

Delputte, P. L., Vanderheijden, N., Nauwynck, H. J. & Pensaert, M. B. (2002). Involvement of the matrix protein in attachment of porcine reproductive and respiratory syndrome virus to a heparinlike receptor on porcine alveolar macrophages. *J Virol* **76**, 4312–4320.

Dewerchin, H. L., Cornelissen, E. & Nauwynck, H. J. (2005). Replication of feline coronaviruses in peripheral blood monocytes. *Arch Virol* **150**, 2483–2500.

Duan, X., Nauwynck, H. J. & Pensaert, M. B. (1997). Effects of origin and state of differentiation and activation of monocytes/macrophages on their susceptibility to porcine reproductive and respiratory syndrome virus (PRRSV). *Arch Virol* **142**, 2483–2497.

González, J. M., Gomez-Puertas, P., Cavanagh, D., Gorbalenya, A. E. & Enjuanes, L. (2003). A comparative sequence analysis to revise the current taxonomy of the family *Coronaviridae*. *Arch Virol* **148**, 2207–2235.

Gorbalenya, A. E., Enjuanes, L., Ziebuhr, J. & Snijder, E. J. (2006). *Nidovirales*: evolving the largest RNA virus genome. *Virus Res* **117**, 17–37.

Hansen, G. H., Delmas, B., Besnardeau, L., Vogel, L. K., Sjöström, H., Laude, H. & Norén, O. (1998). The coronavirus transmissible gastroenteritis virus causes infection after receptor-mediated endocytosis and acid-dependent fusion with an intracellular compartment. *J Virol* **72**, 527–534.

Hohdatsu, T., Okada, S., Ishizuka, Y., Yamada, H. & Koyoma, H. (1992). The prevalence of types I and II feline coronavirus infections in cats. *J Vet Med Sci* **54**, 557–562.

Hohdatsu, T., Izumiya, Y. & Yokoyama, Y. (1998). Differences in virus receptor for type I and type II feline infectious peritonitis virus. *Arch Virol* **143**, 839–850.

Kooi, C., Cervin, M. & Anderson, R. (1991). Differentiation of acid-pH-dependent and -nondependent entry pathways for mouse hepatitis virus. *Virology* **180**, 108–119.

McKeirnan, A. J., Evermann, J. F., Hargis, A., Miller, L. M. & Ott, R. L. (1981). Isolation of feline coronaviruses from two cats with diverse disease manifestations. *Feline Pract* **11**, 16–20.

Morahan, P. S., Connor, J. R. & Leary, K. R. (1985). Viruses and the versatile macrophage. *Br Med Bull* **41**, 15–21.

Nash, T. C. & Buchmeier, M. J. (1997). Entry of mouse hepatitis virus into cells by endosomal and nonendosomal pathways. *Virology* **233**, 1–8.

Nauwynck, H. J., Duan, X., Favoreel, H., Van Oostveldt, P. & Pensaert, M. (1999). Entry of porcine reproductive and respiratory syndrome virus into alveolar macrophages via receptor-mediated endocytosis. *J Gen Virol* **80**, 297–305.

Nomura, R., Kiyota, A., Suzaki, E., Kataoka, K., Ohe, Y., Miyamoto, K., Senda, T. & Fujimoto, T. (2004). Human coronavirus 229E binds to CD13 in rafts and enters the cell through caveolae. *J Virol* **78**, 8701–8708.

Pedersen, N. C., Black, J. W., Boyle, J. F., Evermann, J. F., McKeirnan, A. J. & Ott, R. L. (1983). Pathogenic differences between various feline coronavirus isolates. In *Molecular Biology and Pathogenesis of Coronaviruses*, pp. 365–380. London: Plenum.

Pedersen, N. C., Evermann, J. F., Alison, J., McKeirnan, A. J. & Ott, R. L. (1984). Pathogenicity studies of feline coronavirus isolates 79-1146 and 79-1683. *Am J Vet Res* **45**, 2580–2585.

Rottier, P. J. M., Nakamura, K., Schellen, P., Volders, H. & Haijema, B. J. (2005). Acquisition of macrophage tropism during the pathogenesis of feline infectious peritonitis is determined by mutations in the feline coronavirus spike protein. *J Virol* **79**, 14122–14130.

Savarino, A., Boelaert, J. R., Cassone, A., Majori, G. & Cauda, R. (2003). Effects of chloroquine on viral infections: an old drug against today's diseases? *Lancet Infect Dis* **3**, 722–727.

Spaan, W. J. M., Brian, D., Cavanagh, D., de Groot, R. J., Enjuanes, L., Gorbalenya, A. E., Holmes, K. V., Masters, P. S., Rottier, P. & other authors (2005). Family *Coronaviridae*. In *Virus Taxonomy: Eighth Report of the International Committee on Taxonomy of Viruses*, pp. 947–964. Edited by C. M. Fauquet, M. A. Mayo, J. Maniloff, U. Desselberger & L. A. Ball. San Diego, CA: Elsevier Academic Press.

Stoddart, C. A. & Scott, F. W. (1989). Intrinsic resistance of feline infectious peritoneal macrophages to coronavirus infection correlates with in vivo virulence. *J Virol* **63**, 436–440.

Tresnan, D. B., Levis, R. & Holmes, K. V. (1996). Feline aminopeptidase N serves as a receptor for feline, canine, porcine and human coronaviruses in serogroup I. *J Virol* **70**, 8669–8674.

Vennema, H., Poland, A., Floyd Hawkins, K. & Pedersen, N. C. (1995). A comparison of the genomes of FECVs and FIPVs and what they tell us about the relationships between feline coronaviruses and their evolution. *Feline Pract* **23**, 40–44.

Yeager, C. L., Ashmun, R. A., Williams, R. K., Cardellichio, C. B., Shapiro, L. H., Look, A. T. & Holmes, K. V. (1992). Human aminopeptidase N is a receptor for human coronavirus 229E. *Nature* **357**, 420–422.